Heliyon 9 (2023) e21871

Contents lists available at ScienceDirect

Heliyon

journal homepage: www.cell.com/heliyon

Yinhuapinggan granule ameliorates lung injury caused by multidrug-resistant *Acinetobacter baumannii via* inhibiting NF-κB/NLRP3 pathway

Tianhang Chen [a,1], Haixia Du [a,1], Huifen Zhou [a], Yu He [a], Jiehong Yang [a], Chang Li [a], Chenxing Wei [b], Daojun Yu [b,*], Haitong Wan [a,**]

[a] *Zhejiang Chinese Medical University, Hangzhou, 310053, China*
[b] *Affiliated Hangzhou First People's Hospital, Zhejiang University School of Medicine, Hangzhou, 310006, China*

ARTICLE INFO

Keywords:
A.baumannii
Yinhuapinggan granule
Pneumonia
Inflammatory factors
NF-κB/NLRP3 signaling pathway

ABSTRACT

Yinhuapinggan granule (YHPG) is a traditional Chinese medicine prescription with rich clinical experience for the treatment of colds and coughs. The aim of this study is to investigate the protective effect of YHPG on multidrug-resistant (MDR) *Acinetobacter baumannii* (*A. baumannii*) infection *in vivo* and its potential anti-inflammatory mechanism. BALB/c mice were intranasally inoculated with MDR *A. baumannii* strain to establish the pneumonia infection model, and received intraperitoneally cyclophosphamide to form immunosuppression before attack. YHPG (6, 12 and 18 g/kg) was administered by gavage once a day for 3 consecutive days after infection. The protective effect of YHPG was evaluated by lung index, spleen index, thymus index, pathological changes of lung tissue and inflammatory factors (IL-1β, IL-6 and TNF-α) in serum. The expression of key targets of NF-κB/NLRP3 signaling pathway *in vivo* was analyzed by immunohistochemistry, immunofluorescence, reverse transcription quantitative PCR (RT-qPCR) and Western blot. The results showed that YHPG improved the lung index and its inhibition rate, immune organ indexes and lung pathological changes in infected mice, and significantly reduced IL-1β, IL-6 and TNF-α levels in serum. In addition, YHPG significantly down-regulated the mRNA and protein expression of NF-κB p65, NLRP3, ASC, Caspase-1, TNF-α, IL-6 and IL-1β in mice lung tissue. The results of the current study demonstrated that YHPG has significant protective effects on mice infected with MDR *A.baumannii*, which may be related to the regulation of inflammatory factors and NF-κB/NLRP3 signaling pathway, indicating that YHPG has a wide range of clinical application value and provides a theoretical basis for its treatment of MDR *A.baumannii* infection.

1. Introduction

As a gram-negative bacillus, *Acinetobacter baumannii* has caused serious nosocomial infections and has been identified as a critical

* Corresponding author. Affiliated Hangzhou First People's Hospital, Zhejiang University School of Medicine, 261 Huansha Road, Hangzhou 310006, China.
** Corresponding author. Zhejiang Chinese Medical University, 548 Binwen Road, Hangzhou 310053, China.
E-mail addresses: yudaojun98@163.com (D. Yu), whtong@126.com (H. Wan).
[1] These authors are regarded as co-first authors.

https://doi.org/10.1016/j.heliyon.2023.e21871
Received 11 May 2023; Received in revised form 13 September 2023; Accepted 30 October 2023
Available online 2 November 2023

research and development pathogen by the World Health Organization [1]. *A.baumannii* is easy to cause extensive bacterial infections in hospitals, especially pneumonia, bacteremia and meningitis. In particular, with the increasing detection rate of multidrug-resistant (MDR) and extensively drug-resistant (XDR) *A.baumannii* in recent years, it brings great challenges to global clinical treatment [2]. A recent study published in The Lancet found that 260,000 deaths worldwide in 2019 caused by resistant *A.baumannii* [3]. Especially carbapenem-resistant (CR) *A.baumannii*, during the COVID-19 pandemic, co-infection with SARS-CoV-2 is common and has become a new medical health crisis [4,5].

At present, the treatment of *A.baumannii* infection is very limited, and all known antibiotics have corresponding resistance [6]. More seriously, although tigecycline and polymyxin are the last lines of defense for the treatment of CR *A. baumannii*, there are increasing numbers reports on their related drug resistance in recent years [7,8], and the side effects of the latter on the kidney cannot be ignored [9]. In addition, new treatment methods such as vaccination, iron chelation therapy and phage therapy have unstable clinical efficacy on drug-resistant *A. baumannii*, and the safety problems need to be further found [10–12]. Therefore, it is urgent to develop new effective drug while *A. baumannii* continues to acquire resistance to currently available antibiotics.

The inflammatory response caused by bacteria is the pathogenesis of lower respiratory tract infection, and severe bacterial pneumonia can lead to lung abscess and sepsis, even respiratory failure and shock [13]. A large number of studies have reported that the NF-κB/NLRP3 signaling pathway is involved in the inflammatory response of lung diseases, regulating the activation of inflammasomes and controlling the release of pro-inflammatory factors [14,15]. Therefore, screening effective chemicals to regulate the above signaling pathways may be a considerable therapeutic strategy for the treatment of pneumonia caused by MDR *A.baumannii*.

Compared with the single use of chemical drugs, traditional Chinese medicine (TCM) shows its unexpected drug effect [16]. In response to antibiotic resistance and infectious diseases, TCM has unique advantages of "multi-component, multi-target and multi--effect". Yinhuapinggan granule (YHPG) is composed of *Lonicerae Japonicae Flos, Ephedra Herba*, *Puerariae Lobatae Radix*, *Polygoni Cuspidati Rhizoma*, *Armeniacae Semen Amarum* and *Glycyrrhizae Radix*, which has the effects of heat-clearing and detoxifying, dispersing lung and resolving exterior syndrome. The prescription has obtained the certificate of new drugs of TCM from the National Medical Products Administration (TCM certificate: Z20120004) and production approval (No.2013B00150). But so far, the role and mechanism of YHPG against drug-resistant bacterial infection *in vivo* is not clear. In this study, we evaluated the protective effect of YHPG and explored the possible role of NF-κB/NLRP3 inflammatory signaling pathway in the BALB/c mice model of MDR *A. baumannii*.

2. Materials and methods

2.1. Reagents

YHPG granules (Product batch number: 200201035) were provided from Shaanxi Dongke Pharmaceutical Co., Ltd. (Shaanxi, China), certified by Professor Shengwu Huang, College of Pharmaceutical Science, Zhejiang Chinese Medicine University (Hangzhou, China). According to the quality standards of Chinese Pharmacopoeia (2020 edition), they were ensured that the crude decoction pieces of this batch of tablets met the quality requirements. As reported the previous methods of preparation and quality control of YHPG by our research group, six effective components were detected by high performance liquid chromatography (HPLC) at 254 nm, including chlorogenic acid 13.86 mg/g, amygdalin 22.82 mg/g, polydatin 8.25 mg/g, puerarin 22.93 mg/g, glycyrrhizic acid 4.63 mg/g and emodin 1.32 mg/g (Supplementary Fig. 1).

Tumor necrosis factor alpha (ELISA) kits for IL-1β, IL-6 and TNF-α were obtained from Meibiao Biotechnology (Jiangsu, China). Primary antibodies against IL-1β (ab254360), MPO (ab208670) and GAPDH (ab181602) were purchased from Abcam (Cambridge, MA, USA); Primary antibody against Caspase-1 p20 (SC-398715) was purchased from Santa Cruz Biotechnology (Santa Cruz, CA, USA); Primary antibodies against ASC (CST 15101), NF-κβ p65 (CST 8242), p–NF–κβ p65 (CST 3033) and pro-Caspase-1 (CST 24232) were purchased from Cell Signaling Technology (Danvers, MA, USA); Primary antibody against NLRP3 (NBP2-12446) was purchased from Novus (Littleton, CO, USA). Cyclophosphamide (CY) was purchased from aladdin (Shanghai, China).

2.2. Bacteria

The MDR *A.baumannii* (Supplementary Table 1) used in this study was initially isolated from clinical specimens from the Department of Laboratory Medicine in Hangzhou First People's Hospital, identified by matrix-assisted laser desorption ionization-time of flight mass spectrometry (MALDI-TOF-MS). Antimicrobial susceptibilities of the strain were determined by VITEK-2 Compact analyzer (Biomérieux, France) and the results were interpreted in accordance with the Clinical and Laboratory Standard Institutes (CLSI, 2020) guideline. After whole genome sequencing, the MDR *A.baumannii* strain was inoculated on a blood agar plate and cultured at 37 °C for 24 h. The bacterial suspension was prepared by an electronic turbidimetry using a sterile 0.45 % sodium chloride solution, and then the concentration was adjusted to 2×10^8 CFU/mL.

2.3. Animals

Male specific-pathogen free BALB/c mice (Six-week-old) weighing 22 ± 2 g were provided by Experimental Animal Center, Huazhong University of Science and Technology (Wuhan, China). All mice were housed in individually ventilated cages in negative pressure barrier environment, free access to food and water under conditions with the temperature at 24 ± 2 °C, the relative humidity of 57 ± 3 %, and a 12 h light/darkness cycle. In addition, the animal experiments in this study were protected according to the relevant

Table 1
Sequences of primers for RT-qPCR analysis.

Gene	Primer sequence (5'→3')	Size (bp)
IL-1β	GGCAGGCAGTATCACTCATTGTG GCTCATGTCCTCATCCTGGAAG	89
IL-6	TCTACTCGGCAAACCTAGTGCGTTA TTCTGACCACAGTGAGGAATGTCCA	70
TNF-α	GACCCTCACACTCAGATCATCTTCT GCTACGACGTGGGCTACAG	63
NF-κB p65	TCAATGGCTACACAGGACCA TCGCTTCTTCACACACTGGA	185
NLRP3	GCAGGCATCGGGAAAACC CTCTCGGCAGTGGATAAAGAACAAA	108
Caspase-1	GGGACCTATGTGATCATGTCTCT CTGCCAGGTAGCAGTCTTCA	90
ASC	GGTCACAGAAGTGGACGGAGTG CATCTTGTCTTGGCTGGTGGTCT	103
GADPH	GAAGGTCGGTGTGAACGGATTTG CATGTAGACCATGTAGTTGAGGTCA	127

regulations of the Experimental Animal Center in Huazhong University of Science and Technology, and approved by the Ethics Committee (NO. S2901).

2.4. Preparation of infection model and YHPG treatment

The mice were randomly divided into five groups: control group, model group, YHPG low-dose group (6 g/kg), YHPG middle-dose group (12 g/kg) and YHPG high-dose group (18 g/kg). Before infection with *A.baumannii*, all mice were intraperitoneally injected with 100 mg/kg and 150 mg/kg CY on the first and fourth days to form an immunosuppressive state. After that, the mice were placed in a sealed isolation box, and the multi-channel small animal anesthesia ventilator was started. After mild anesthesia with isoflurane, the mice in the model group and the administration group were infected with 2×10^8 CFU/mL bacterial suspension by nasal drip (50 μL), and the remaining mice were given an equal amount of physiological saline by nasal drip. After infection, the mice in the treatment group were intragastrically administered with YHPG (0.01 mL/g) of corresponding concentration once a day for 5 consecutive days. Mice in control group and model group were given the same amount of physiological saline at the same time. In our experiment, the dose of YHPG (6, 12 and 18 g/kg) administered to mice was equivalent to the clinical adult dose (once, twice and three times) calculated according to the body surface area of animals. Finally, all mice were sacrificed on the sixth day after infection.

2.5. ELISA

The mice were fixed and the eyeballs were removed to collect blood. When the blood ran out, the mice were sacrificed by dislocation. The blood samples were centrifuged at 3000×*g* at 4 °C for 15 min, used to determine the serum inflammatory cytokine levels (TNF-α, IL-6 and IL-1β) according to ELISA kit from manufacturer's instructions. Finally, the absorbance was detected at 450 nm using a microplate reader.

2.6. Determination of organ index

The lung, thymus and spleen were removed from the chest cavity and abdominal cavity respectively by surgery. These tissues were washed with physiological saline and dried with filter paper, and finally weighed. Inhibition radio of lung index and organ index were calculated according to the following formula:

$$\text{Inhibition ratio of lung index} = (\text{A - B})/\ \text{A}$$

A:average lung index of bacterial infection control group

B:average lung index of experimental control group

$$\text{Organ index} = \text{Organ weight}/\text{Body weight} \times 100\%$$

2.7. Histopathological evaluation

The lung tissues of mice in different groups were taken, rinsed with physiological saline and fixed in 4 % paraformaldehyde solution for 48 h, dehydrated with ethanol, embedded in paraffin, and then cut into 4-μm slices. After hematoxylin impregnating and eosin staining, the pathological changes of lung tissues were observed under a BX60 optical microscope (Olympus, Japan).

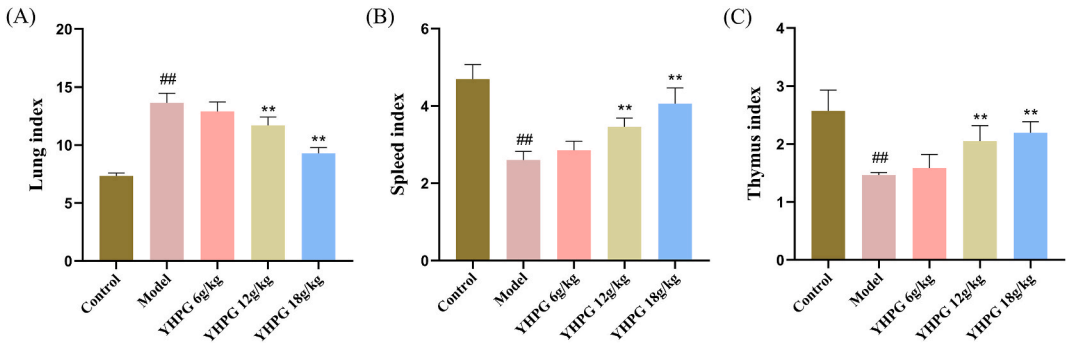

Fig. 1. The change of organ indexes in MDR *A.baumannii* infected mice treated with YHPG. (A) Lung index; (B) Spleed index; (C) Thymus index. Mean ± SD (n = 6). $^{\#\#}P < 0.01$ vs control group; $^{**}P < 0.01$ vs model group.

2.8. RT-qPCR analysis

Total RNA was extracted from lung tissue of mice using TRIzol® Reagent Plus RNA Purification Kit (Thermo Fisher, Waltham, USA). Then the total RNA was reverse transcribed to cDNA using SuperScript^{TM}III First-Strand Synthesis SuperMix (Thermo Fisher, Waltham, USA). RT-qPCR was performed using Power SYBR® Green PCR Master Mix (Applied Biosystems, Waltham, USA). The experimental reaction conditions follow these steps: 95 °C for 1 min, follow by 40 cycles of 95 °C for 15 s, 63 °C for 25 s. The primers (Table 1) for the amplification were designed and synthesized by Shanghai Sangon Bioengineering Co., Ltd. The experimental detection and analysis were used for a CFX384 real-time PCR detection system (Bio-Rad, USA). GAPDH was used as the reference gene to quantify the relative expression of the target gene according to the $2^{-\Delta\Delta Ct}$ method.

2.9. Immunohistochemistry analysis

As mentioned above, the 4-μm slices after paraffin embedding and cutting were dewaxed in xylene, ethanol gradient hydration, antigen retrieval under high temperature and high pressure, and 3 % hydrogen peroxide aqueous blocking endogenous peroxidase. Subsequently, the lung sections were incubated with primary antibodies against MPO (1:800) and NF-κB p65 (1:400) respectively at room temperature for 60 min, and then incubated with horseradish-peroxidase (HRP) conjugated secondary antibody (EnVision Two-Step kit, Beijing, China) at room temperature for 30 min. After hematoxylin counterstaining, it was developed with diaminobenzidine (DAB), dehydrated with ethanol, transparentized with xylene, and finally observed under the optical microscope. The positive staining was represented by brown-yellow products and evaluated by Immunoreactivity Score.

2.10. Immunofluorescence staining

After dewaxing, the pretreated lung tissue sections were incubated with NLRP3 primary antibody (1: 50) at 37 °C for 60 min. Then the sections were incubated with FITC-conjugated secondary antibody for 30 min, counterstained with 0.1 % 4',6-diamidino-2-phenylindole (DAPI) and finally sealed with glycerol. The fluorescence images were observed and photographed using an Axio Observer A1 fluorescence microscope (ZEISS, Germany) and the fluorescence intensity was analyzed using Image J software.

2.11. Western blot assay

RIPA Buffer (Thermo Fisher, Waltham, USA) was used to extract the total protein of lung tissue samples, and then the total protein was quantified by the bicinchoninic acid (BCA) quantitative kit (Beyotime, Beijing, China). 60 μg of total protein sampels were added to sodium dodecyl sulfate-polyacrylamide gel electrophoresis (SDS-PAGE) for denaturation and separation, and transferred to polyvinylidene difluoride (PVDF) membranes by electrophoresis. The membranes were blocked with 5 % BSA at room temperature for 60 min. After being washed, they were incubated with the corresponding primary antibodies: ASC (1:1000), NLRP3 (1:500), NF-κB p65 (1:1000), p–NF–κB p65 (1:1000), pro-Caspase-1 (1:1000), Caspase-1 p20 (1:200), IL-1β (1:500) or GADPH (1:10000) at 4 °C overnight. Afterwards, the membranes were incubated with HRP-conjugated secondary antibodies at room temperature for 90 min. By enhanced chemiluminescence reagent (ECL) exposure and visualization, the band gray was calibrated by Image J software. GAPDH was used as an internal reference for quantitative analysis of the target band to detect the relative expression of the protein.

2.12. Statistical analysis

The experimental data were analyzed and plotted by SPSS 20.0 software and GraphPad Prism 8.0 software, and the statistical significance between groups was analyzed by one-way analysis of variance (ANOVA). The results were expressed as mean ± standard deviation (Mean ± SD), when P value < 0.05 for the difference was statistically significant.

Table 2
The inhibition rate of lung index in MDR *A.baumannii* infected mice treated with YHPG.

Group	Dose (g/kg)	Inhibition rate of lung index (%)
Control	–	–
Model	–	–
YHPG	6	5.39
YHPG	12	14.16
YHPG	18	31.90

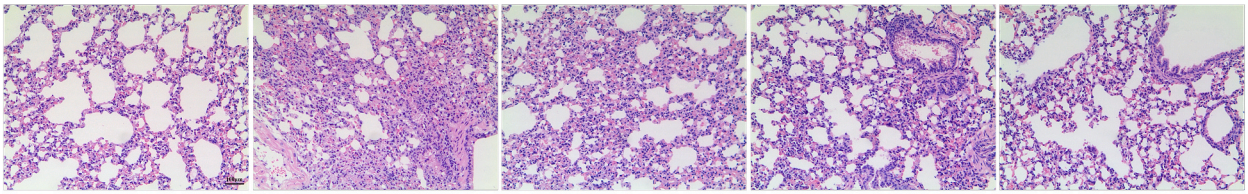

Fig. 2. Effects of YHPG on pulmonary pathological alterations induced by MDR *A.baumannii*. (A–E) Pathological photos of each group under microscope (magnification 100 ×).

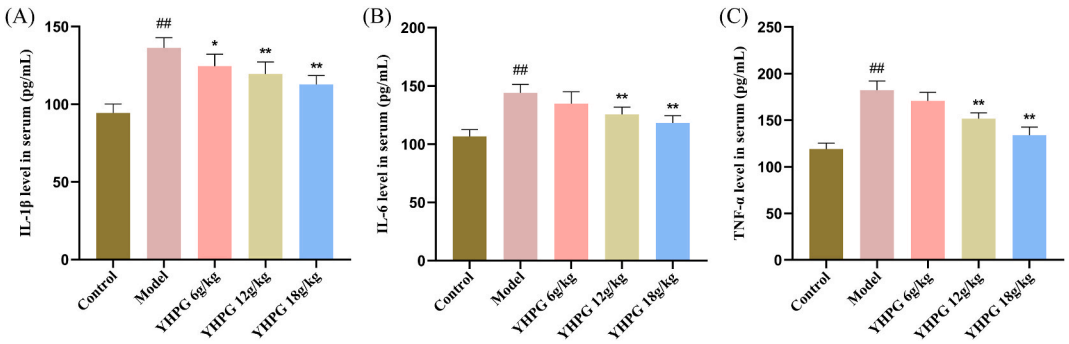

Fig. 3. The levels of inflammatory cytokines of (A) IL-1β, (B) IL-6 and (C) TNF-α in serum. Mean ± SD (n = 6), $^{\#\#}P < 0.01$ vs control group; $^{*}P < 0.05$, $^{**}P < 0.01$ vs model group.

3. Results

3.1. YHPG improves organ indexes in mice with MDR A.baumannii

In this experiment, we established a bacterial pneumonia model in mice induced by intranasal drip of MDR *A.baumannii*. Lung index and its inhibition ratio were calculated to evaluate pulmonary edema, and immune organ indiexes were used to evaluate immune function. As shown in Fig. 1 and Table 2, the lung index of the infected model group was significantly higher than that of the control group after MDR *A.baumannii* infection ($P < 0.01$). Lung index was decreased and inhibition rate of lung index was increased after treatment with different doses of YHPG that there was significant difference between 12 and 18 g/kg. In addition, the spleen index and thymus index of YHPG (12 and 18 g/kg) were significantly higher than those of the model group ($P < 0.01$), while YHPG (6 g/kg) had no significant effect on all the above organ indexes ($P > 0.05$). Therefore, the results suggest that YHPG (12 and 18 g/kg) can improve pulmonary edema and regulate immune organ indexes to inhibit pneumonia caused by MDR *A.baumannii*.

3.2. YHPG alleviated lung injury induced by MDR A.baumannii

The pathological images of lung tissue in mice were observed by an optical microscope. As shown in Fig. 2, after infection with MDR *A.baumannii*, the changes showed the alveolar was not only structural destroyed and blurred, but also irregularly enlarged and thickened in wall, as well as inflammatory cell infiltration in the pulmonary interstitial and alveolar. Compared with the model group, each group after YHPG treatment can improve lung tissue injury to varying degrees, the degree of injury was significantly reduced, and the range of lesions was significantly reduced. The above revealed that YHPG could improve the pathological conditions such as alveolar wall thickening and alveolar injury.

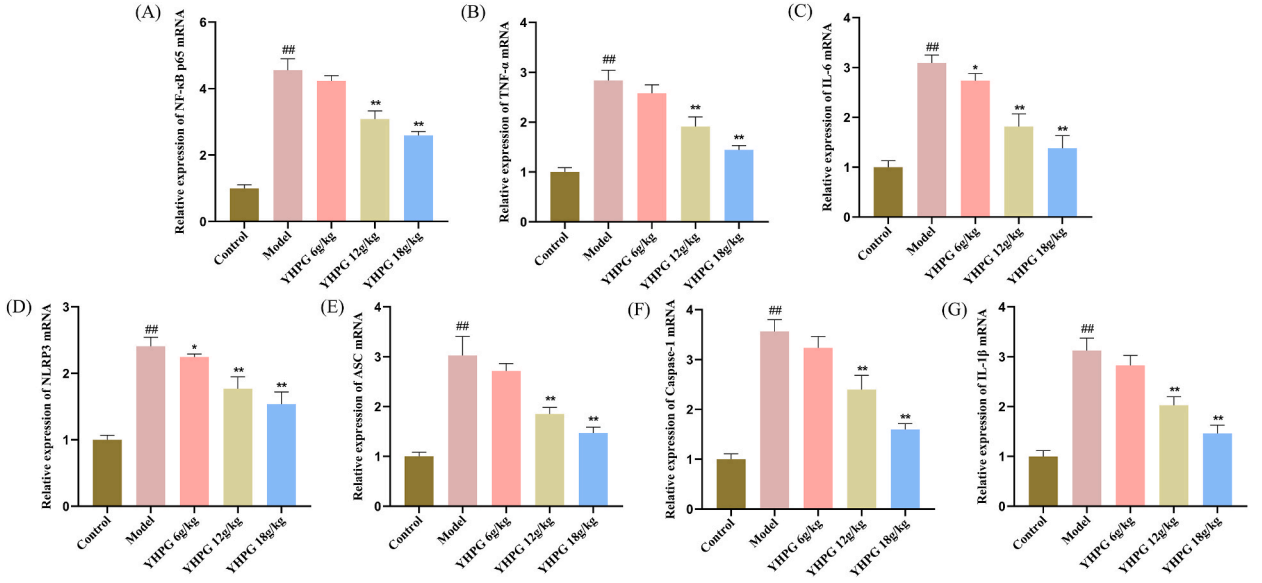

Fig. 4. Effects of YHPG on the mRNA expression of (A) NF-κB p65, (B) TNF-α, (C) IL-6, (D) NLRP3, (E) ASC, (F) Caspase-1 and (G) IL-1β in lung tissue of mice infected with MDR *A.baumannii*. Mean ± SD (n = 6). $^{\#\#}P < 0.01$ vs control group; $^{*}P < 0.05$, $^{**}P < 0.01$ vs model group.

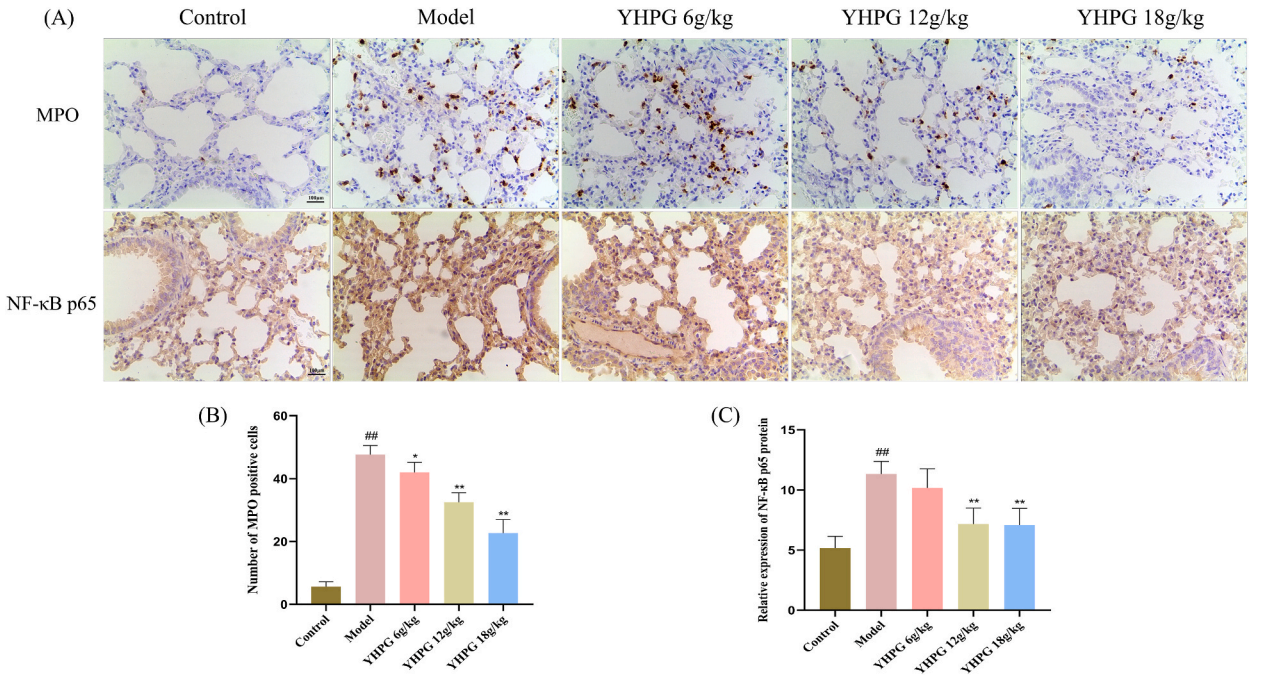

Fig. 5. Effects of YHPG on the protein expression of MPO and NF-κB p65 in MDR *A.baumannii* infected mice. (A) Immunostaining microscopy of MPO and NF-κB p65 in lung tissue of mice (magnification 200 ×). (B, C) Immunohistochemical analysis of MPO and NF-κB p65 in lung tissue of mice infected with MDR *A.baumannii*. Mean ± SD (n = 6). $^{\#\#}P < 0.01$ vs control group; $^{*}P < 0.05$, $^{**}P < 0.01$ vs model group.

3.3. YHPG regulates the levels of IL-6, IL-1β and TNF-α in serum of mice infected with MDR A.baumannii

The regulatory effect of YHPG on cytokine secretion was evaluated. As shown in Fig. 3, compared with the control group, the levels of IL-1β, IL-6 and TNF-α in the serum of the model group were significantly increased ($P < 0.01$). After administration of 12 and 18 g/kg YHPG, the levels of TNF-α and IL-6 were significantly lower than those in the model group ($P < 0.01$). Administration of 6, 12 and 18 g/kg YHPG significantly reduced the level of IL-1β in comparison with the model group ($P < 0.01$, $P < 0.05$).

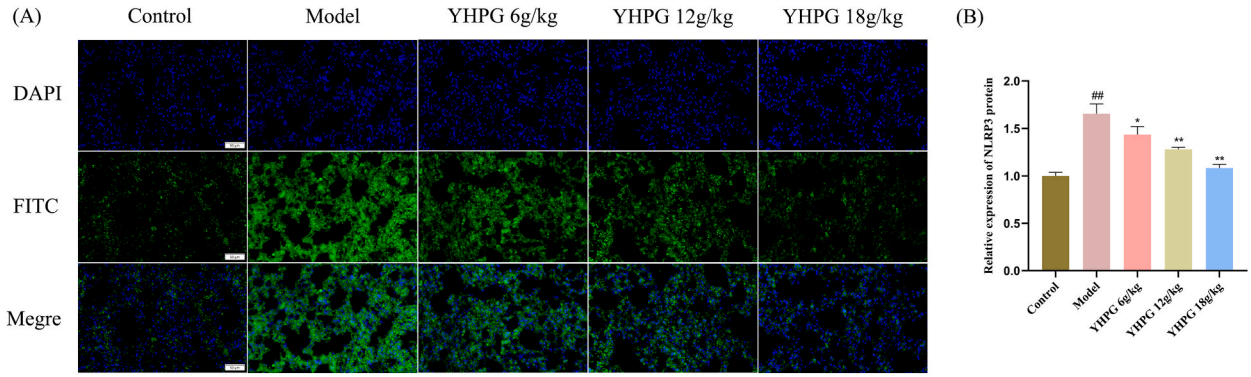

Fig. 6. (A) Representative images of NLRP3 immunofluorescence staining after MDR *A.baumannii* infection. (B) Quantitative analysis of NLRP3 fluorescence intensity (Bar = 50 μm). Mean ± SD (n = 3). $^{\#\#}P < 0.01$ vs control group; $^{*}P < 0.05$, $^{**}P < 0.01$ vs model group.

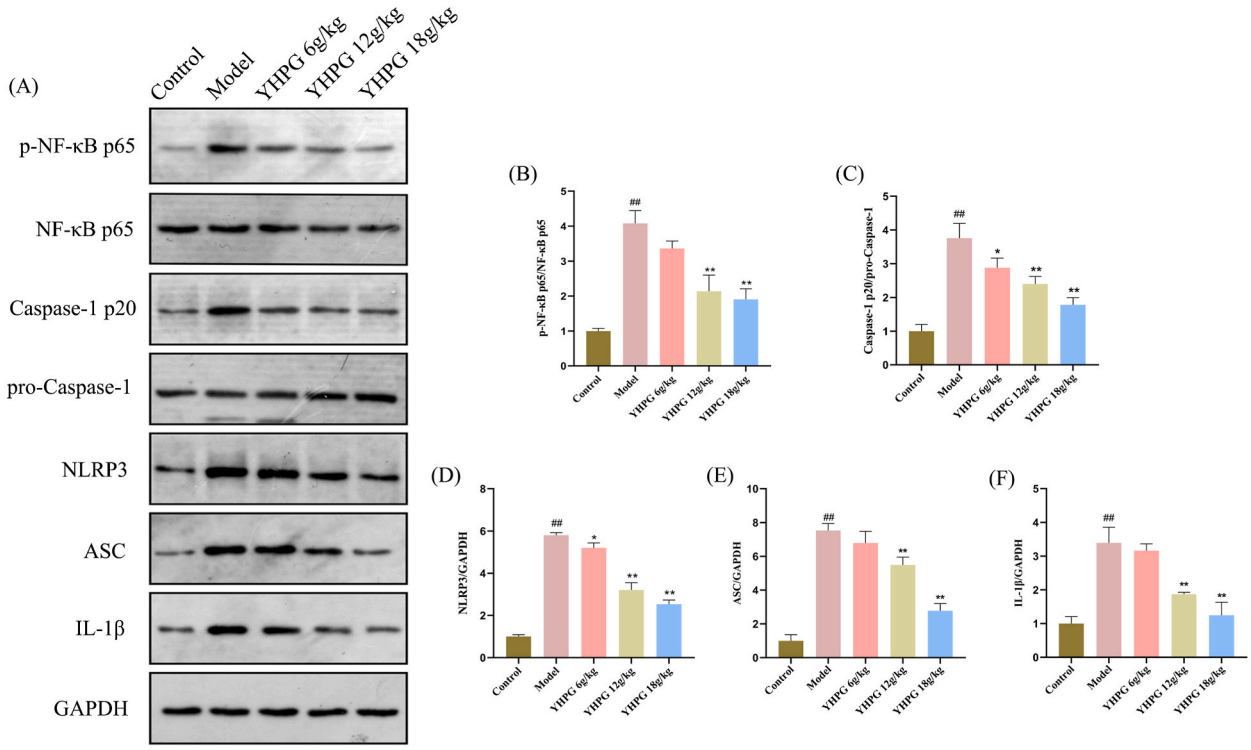

Fig. 7. Effects of YHPG on protein expression of key targets of NF-κB/NLRP3 pathway in lung tissue of mice infected with MDR *A.baumannii*. (A) Representative images of Western blot showing the NF-κB/NLRP3 pathway-related proteins. (B–F) Semi-quantitative analysis of NF-κB/NLRP3 pathway-related protein expression. Mean ± SD (n = 3). $^{\#\#}P < 0.01$ vs control group; $^{*}P < 0.05$, $^{**}P < 0.01$ vs model group.

3.4. YHPG regulated the mRNA expression of inflammation-related genes in lung tissue of mice infected with MDR A.baumannii

In order to evaluate the effect of YHPG on various inflammatory pathways caused by bacterial infection, the expression of key target genes in NF-κB/NLRP3 signaling pathway was detected. As shown in Fig. 4, the mRNA expression of NF-κB p65, NLRP3, ASC, Caspase-1, IL-1β, IL-6 and TNF-α in lung tissue after infection was significantly elevated in comparison with the control group. In addition, compared with the model group, YHPG (6, 12 and 18 g/kg) could significantly reduce the mRNA expression of NLRP3 and IL-6 ($P < 0.01$, $P < 0.05$), and YHPG (12 and 18 g/kg) significantly reduced the mRNA expression of NF-κB p65, ASC, Caspase-1, IL-1β and TNF-α ($P < 0.01$). These results confirmed that YHPG regulated the mRNA expression of NF-κB p65, NLRP3, ASC, Caspase-1, IL-1β, IL-6 and TNF-α, which are key targets of inflammatory signaling pathway of lung tissue in mice infected with MDR *A.baumannii*.

3.5. Effects of YHPG on MPO and NF-κB p65 expression in lung tissue of mice infected with MDR A.baumannii by immunohistochemistry

In order to further explore the pathological changes of lung inflammation in each group, MPO and NF-κB p65 in lung tissue were determined by immunohistochemistry to determine whether YHPG regulated the expression of these proteins. MPO is mainly expressed in the cytoplasm of neutrophils infiltrated in the lung, while NF-κB p65 is diffusely expressed in the cytoplasm of airway epithelial cells, tissue phagocytes, vascular endothelial cells and inflammatory cells. As shown in Fig. 5, the number of MPO positive cells and the expression of NF-κB p65 protein in the model group were significantly higher than those in the control group ($P < 0.01$). Compared with the model group, YHPG (6, 12 and 18 g/kg) treatment groups significantly decreased the number of MPO positive cells ($P < 0.01$, $P < 0.05$), and YHPG (12 and 18 g/kg) treatment groups significantly down-regulated the protein expression of NF-κB p65 ($P < 0.01$).

3.6. Effect of YHPG on NLRP3 expression in lung tissue of mice infected with MDR A.baumannii by immunofluorescence

The NLRP3 inflammasome triggers an inflammatory response during bacterial pneumonia. In order to clarify whether the possible anti-inflammatory mechanism of YHPG is related to NLRP3, we detected the protein expression of NLRP3 in lung tissue by immunofluorescence. As shown in Fig. 6, compared with the control group, the expression of NLRP3 in the lung tissue of mice infected with MDR *A.baumannii* increased significantly ($P < 0.01$). The protein expression of NLRP3 in YHPG (6, 12 and 18 g/kg) treatment groups were significantly lower than that in model group ($P < 0.01$, $P < 0.05$). The above observations suggest that YHPG may inhibit the activation of NLRP3 inflammasome after MDR *A.baumannii* infection.

3.7. Effects of YHPG on protein expression of key targets of NF-κB/NLRP3 pathway in lung tissue of mice infected with MDR A.baumannii

It is well known that NF-κB plays an important role in the response to inflammatory stress and NLRP3 activation. Based on the above experimental results, we speculated that YHPG might be involved in the regulation of target proteins related to NF-κB/NLRP3 signaling pathway. The protein expression levels of p–NF–κB p65, NF-κB p65, NLRP3, ASC, IL-1β, pro-Caspase-1 and Caspase-1 p20 were further explored by Western blot analysis. As shown in Fig. 7, compared with the control group, the levels of p–NF–κB p65, NLRP3, ASC, IL-1β and Caspase-1 p20 in the lung tissue of the model group were significantly increased ($P < 0.01$). Compared with the model group, YHPG (12 and 18 g/kg) treatment groups decreased significantly the protein expression of p–NF–κB p65, ASC and IL-1β ($P < 0.01$), and YHPG (6, 12 and 18 g/kg) treatment groups reduced significantly the protein expression of NLRP3 and Caspase-1 p20 ($P < 0.01$, $P < 0.05$). It can be seen that YHPG can reduce the phosphorylation of p65, restrained the nuclear translocation of NF-κB, inhibit the activation of inflammasomes, and thereby down-regulating the production of proinflammatory cytokines, ultimately alleviating the inflammatory response. Overall, the results suggest that YHPG may be involved in regulating the activation of the NF-κB/NLRP3 pathway to exert a protective effect.

4. Discussion

A.baumannii had become one of the important pathogens of hospital-associated infection, especially hospital-acquired pneumonia (HAP) and ventilator-associated pneumonia (VAP) [17]. Although HAP caused by *A.baumannii* was a common clinical phenomenon, the mortality of VAP and community-acquired pneumonia (CAP) caused by it was from 35 % to 64 % [18,19]. It is reported that the resistance of non-fermenting Gram-negative bacteria such as *A.baumannii* to commonly used antibiotics has remained at a high level year by year [20]. With the widespread use of antibiotics, the emergence of multidrug-resistant and even pan-resistant *A.baumannii* have made the form of clinical treatment more severe, which has been recognized as one of the major threats of this century [21]. In addition, the range of antibiotics available is very limited, which makes effective antibiotics gradually fall into an invalid dilemma.

Chinese herbal medicine is an indispensable core of the development system of traditional Chinese medicine. Because of its affordable price, small side effects and multi-target treatment, it has unique advantages in the prevention and treatment of infectious diseases and has been widely recognized in China and other Asian countries [22,23]. YHPG is a good prescription developed by Professor Haitong Wan based on the TCM pathogenesis and years of clinical experience in the treatment of pneumonia. Our previous study found that YHPG has antiviral and antibacterial effects [24–26], which lays a foundation for further *in vivo* research. Therefore, in this experiment, we verified the therapeutic effect of YHPG on MDR *A.baumannii* induced pneumonia in mice and further explored its possible mechanism of regulating inflammatory response.

In this study, the pneumonia model in mice induced by MDR *A.baumannii* presented typical pathophysiological changes [27]. The pathological results showed thickening of the alveolar wall and exudation of inflammatory cells in infected mice. The degree of change in lung index is one of the common used indicators to characterize lung tissue injury, and the ratio of spleen and thymus to body weight can initially reflect the immune function of the body [28]. After YHPG (12 and 18 g/kg) treatment, the lung index of mice decreased, the spleen index and thymus index increased, and the above lesions were reversed, suggesting that YHPG may exert the immune function of immune organs, enhance the body's immunity against MDR *A.baumannii*, and then reduce lung injury.

It is well known that inflammation is the body's self-defense response to bacterial invasion, but excessive inflammatory response is the main factor causing lung injury [29]. Complex cytokines mediate cytokine storms and induce inflammatory responses [30]. After the infection of MDR *A.baumannii*, pro-inflammatory cytokines such as IL-1β, IL-6 and TNF-α were produced and released, and neutrophils were recruited to accumulate and infiltrate in the pulmonary interstitial and alveolar space, rapidly engulfing and eliminating MDR *A.baumannii* [31,32]. MPO activity is an indicator of neutrophil infiltration of inflammatory and damaged tissues [33]. It was

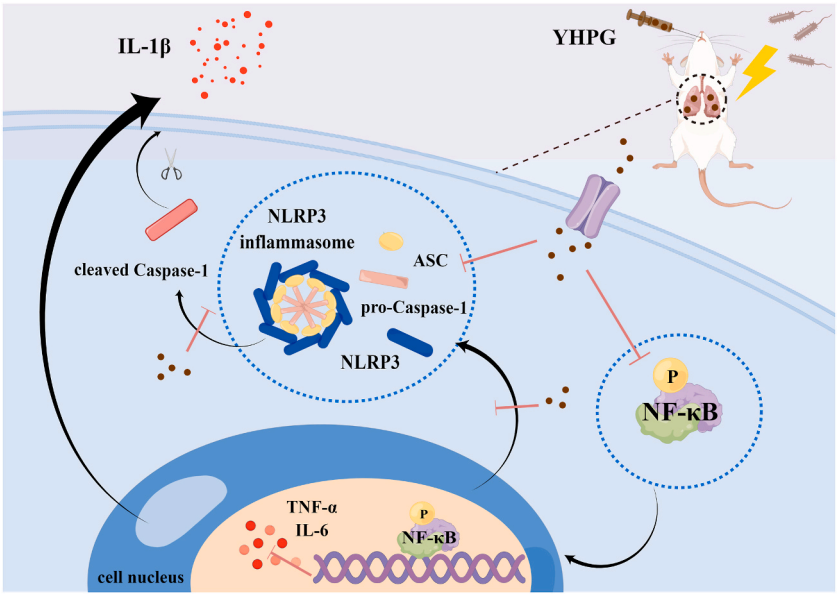

Fig. 8. The molecular mechanism of the protective effect of YHPG on pneumonia caused by MDR *A.baumanni* was shown. MDR *A.baumanni* stimulates NF-κB phosphorylation and inflammasome activation by activating the signaling pathway of NF-κB/NLRP3, thereby promoting the production of TNF-α, IL-6 and IL-1β in lung tissue, leading to severe inflammation. Severe inflammatory response causes congestion and edema of lung tissue, leading to lung injury. YHPG can reverse these destructive effects and reduce lung inflammation.

found that YHPG dose-dependently reduced the production of IL-1β, IL-6, TNF-α and MPO induced by MDR *A.baumannii*, controlled the excessive inflammation, maintained the stability of the internal environment of the lungs, and thus protected the body.

NLRP3 inflammasome plays an important role in humans and rodents against pathogens such as invasive bacteria and in the activation and maturation of IL-1β [34]. Among them, NLRP3 inflammasome is a protein complex composed of three protein subunits: receptor protein NLRP3, effector protein pro-Caspase-1 and adaptor protein ASC [35]. The activation of inflammasome is mediated by two key signals. First, bacterial stimulation causes the release of NF-κB dimers, and activated p65 nuclear transport binds DNA, which is a key role of NF-κB signaling, and then further induces the expression of NLRP3, Caspase-1 and IL-1β [36]. The second signal can be activated by a series of stimuli, including pathogenic microorganisms and bacterial toxins, leading to inflammasome assembly and Caspase-1 activation [37]. NLRP3 protein is activated and oligomerized, recruited and bound to ASC, some of which cleave pro-Caspase-1 into its active isomer Caspase-1, and then the activated Caspase-1 processes and releases mature IL-1β and IL-18, secreting these inflammatory cytokines into the extracellular space and amplifying an inflammatory response [38,39]. In this study, we used RT-qPCR, immunohistochemistry, immunofluorescence and Western blot to explore the above potential mechanisms of YHPG's protective effect on pneumonia caused by MDR *A.baumannii* infection. The results showed that YHPG (12 and 18 g/kg) significantly reduced the expression of p–NF–κB p65, NLRP3, ASC, Caspase-1 p20 and IL-1β induced by MDR *A.baumanni*, indicating that YHPG could inhibit the activation of inflammasome by regulating the NF-κB/NLRP3 signaling pathway, thereby inhibiting the expression of pro-inflammatory factors such as IL-1β, IL-6 and TNF-α and alleviating the lung inflammation induced by MDR *A. baumannii*.

In general, our study has confirmed that MDR *A.baumanni* can activate the NF-κB/NLRP3 pathway, promote the up-regulation of a series of pro-inflammatory cytokines, and then produce and aggravate lung injury. YHPG can reduce pulmonary edema, increase immune organ function, regulate cytokine production, and improve the pathological process of pneumonia caused by MDR *A.baumanni*. The possible mechanism of YHPG protecting pneumonia caused by MDR *A.baumanni* is to down-regulate the secretion of IL-1β, TNF-α and IL-6 by inhibiting the NF-κB/NLRP3 pathway (Fig. 8).

Collectively, the results showed that YHPG had a protective effect on bacterial pneumonia induced by MDR *A.baumannii* in mice. The antibacterial effect of YHPG may be related to the inhibition of NF-κB/NLRP3 signaling pathway. Our study reveals that YHPG may be a candidate drug for the treatment of bacterial pneumonia. However, the present study has its limitations. One limitation is that although we found that YHPG can reduce inflammation in lung injury of mice infected with MDR *A.baumannii*, whether it affects the drug resistance mechanism of *A.baumannii* still needs further exploration and research. Another limitation is that we need to do more experiments (such as subjects of different ages or physiological states) to explore whether YHPG can completely alleviate the symptoms and inflammatory indicators of mice infected with MDR *A.baumannii*.

Author contribution statement

Tianhang Chen, Haixia Du: Performed the experiments; Analyzed and interpreted the data; Wrote the paper. Huifen Zhou, Yu He, Jiehong Yang: Analyzed and interpreted the data; Contributed reagents, materials, analysis tools or data. Chang Li, Chenxing Wei:

Performed the experiments. Haitong Wan, Daojun Yu: Conceived the idea and designed the experiments; Contributed reagents, materials, analysis tools or data.

Data availability statement

Data will be made available on request.

Funding

This work was financially supported by National Natural Science Foundation of China (No.81930111), the administration of Traditional Chinese Medicine of Zhejiang Province of China (No. 2023ZR010) and the Research Project of Zhejiang Chinese Medical University (No. 2021RCZXZK22).

Declaration of competing interest

The authors declare that they have no known competing financial interests or personal relationships that could have appeared to influence the work reported in this paper.

Appendix A. Supplementary data

Supplementary data to this article can be found online at https://doi.org/10.1016/j.heliyon.2023.e21871.

References

[1] E. Tacconelli, E. Carrara, A. Savoldi, S. Harbarth, M. Mendelson, D.L. Monnet, et al., Discovery, research, and development of new antibiotics: the WHO priority list of antibiotic-resistant bacteria and tuberculosis, Lancet Infect. Dis. 18 (3) (2018) 318–327, https://doi.org/10.1016/S1473-3099(17)30753-3.
[2] S.S. Kanj, M. Bassetti, P. Kiratisin, C. Rodrigues, M.V. Villegas, Y. Yu, et al., Clinical data from studies involving novel antibiotics to treat multidrug-resistant Gram-negative bacterial infections, Int. J. Antimicrob. Agents 60 (3) (2022), 106633, https://doi.org/10.1016/j.ijantimicag.2022.106633.
[3] C.J.L. Murray, K.S. Ikuta, F. Sharara, L. Swetschinski, G. Robles Aguilar, A. Gray, et al., Global burden of bacterial antimicrobial resistance in 2019: a systematic analysis, Lancet 399 (10325) (2022) 629–655, https://doi.org/10.1016/S0140-6736(21)02724-0.
[4] I. Kyriakidis, E. Vasileiou, Z.D. Pana, A. Tragiannidis, Acinetobacter baumannii antibiotic resistance mechanisms, Pathogens 10 (3) (2021) 373, https://doi.org/10.3390/pathogens10030373.
[5] C.C. Lai, S.Y. Chen, W.C. Ko, P.R. Hsueh, Increased antimicrobial resistance during the COVID-19 pandemic, Int. J. Antimicrob. Agents 57 (4) (2021), 106324, https://doi.org/10.1016/j.ijantimicag.2021.106324.
[6] A.Y. Peleg, H. Seifert, D.L. Paterson, Acinetobacter baumannii: emergence of a successful pathogen, Clin. Microbiol. Rev. 21 (3) (2008) 538–582, https://doi.org/10.1128/CMR.00058-07.
[7] T.P. Lim, R.T. Ong, P.Y. Hon, J. Hawkey, K.E. Holt, T.H. Koh, et al., Multiple genetic mutations associated with polymyxin resistance in acinetobacter baumannii, Antimicrob. Agents Chemother. 59 (12) (2015) 7899–7902, https://doi.org/10.1128/AAC.01884-15.
[8] W. Ni, Y. Han, J. Zhao, C. Wei, J. Cui, R. Wang, et al., Tigecycline treatment experience against multidrug-resistant Acinetobacter baumannii infections: a systematic review and meta-analysis, Int. J. Antimicrob. Agents 47 (2) (2016) 107–116, https://doi.org/10.1016/j.ijantimicag.2015.11.011.
[9] J. Wang, H. Niu, R. Wang, Y. Cai, Safety and efficacy of colistin alone or in combination in adults with Acinetobacter baumannii infection: a systematic review and meta-analysis, Int. J. Antimicrob. Agents 53 (4) (2019) 383–400, https://doi.org/10.1016/j.ijantimicag.2018.10.020.
[10] J.M. Knisely, B. Liu, R.T. Ranallo, L. Zou, Vaccines for healthcare-associated infections: promise and challenge, Clin. Infect. Dis. 63 (5) (2016) 657–662, https://doi.org/10.1093/cid/ciw333.
[11] C. Rohde, G. Resch, J.P. Pirnay, B.G. Blasdel, L. Debarbieux, D. Gelman, et al., Expert opinion on three phage therapy related topics: bacterial phage resistance, phage training and prophages in bacterial production strains, Viruses 10 (4) (2018) 178, https://doi.org/10.3390/v10040178.
[12] V. Vinuesa, M.J. McConnell, Recent advances in iron chelation and gallium-based therapies for antibiotic resistant bacterial infections, Int. J. Mol. Sci. 22 (6) (2021) 2876, https://doi.org/10.3390/ijms22062876.
[13] R.L. Kradin, S. Digumarthy, The pathology of pulmonary bacterial infection, Semin. Diagn. Pathol. 34 (6) (2017) 498–509, https://doi.org/10.1053/j.semdp.2017.06.001.
[14] K.S. Alharbi, N.K. Fuloria, S. Fuloria, S.B. Rahman, W.H. Al-Malki, M.A. Javed Shaikh, et al., Nuclear factor-kappa B and its role in inflammatory lung disease, Chem. Biol. Interact. 345 (2021), 109568, https://doi.org/10.1016/j.cbi.2021.109568.
[15] M. Sayan, B.T. Mossman, The NLRP3 inflammasome in pathogenic particle and fibre-associated lung inflammation and diseases, Part. Fibre Toxicol. 13 (1) (2016) 51, https://doi.org/10.1186/s12989-016-0162-4.
[16] T. Su, Y. Qiu, X. Hua, B. Ye, H. Luo, D. Liu, et al., Novel opportunity to reverse antibiotic resistance: to explore traditional Chinese medicine with potential activity against antibiotics-resistance bacteria, Front. Microbiol. 11 (2020), 610070, https://doi.org/10.3389/fmicb.2020.610070.
[17] S. Mohd Sazlly Lim, A. Zainal Abidin, S.M. Liew, J.A. Roberts, F.B. Sime, The global prevalence of multidrug-resistance among Acinetobacter baumannii causing hospital-acquired and ventilator-associated pneumonia and its associated mortality: a systematic review and meta-analysis, J. Infect. 79 (6) (2019) 593–600, https://doi.org/10.1016/j.jinf.2019.09.012.
[18] L.C. Antunes, P. Visca, K.J. Towner, Acinetobacter baumannii: evolution of a global pathogen, Pathog. Dis. 71 (3) (2014) 292–301, https://doi.org/10.1111/2049-632X.12125.
[19] C. Dexter, G.L. Murray, I.T. Paulsen, A.Y. Peleg, Community-acquired Acinetobacter baumannii: clinical characteristics, epidemiology and pathogenesis, Expert Rev. Anti Infect. Ther. 13 (5) (2015) 567–573, https://doi.org/10.1586/14787210.2015.1025055.
[20] F. Hu, D. Zhu, F. Wang, M. Wang, Current status and trends of antibacterial resistance in China, Clin. Infect. Dis. 67 (suppl_2) (2018) S128–S134, https://doi.org/10.1093/cid/ciy657.
[21] C. Willyard, The drug-resistant bacteria that pose the greatest health threats, Nature 543 (7643) (2017) 15, https://doi.org/10.1038/nature.2017.21550.
[22] K. Huang, P. Zhang, Z. Zhang, J.Y. Youn, C. Wang, H. Zhang, et al., Traditional Chinese Medicine (TCM) in the treatment of COVID-19 and other viral infections: efficacies and mechanisms, Pharmacol. Ther. 225 (2021), 107843, https://doi.org/10.1016/j.pharmthera.2021.107843.

[23] Y. Ma, M. Chen, Y. Guo, J. Liu, W. Chen, M. Guan, et al., Prevention and treatment of infectious diseases by traditional Chinese medicine: a commentary, APMIS 127 (5) (2019) 372–384, https://doi.org/10.1111/apm.12928.
[24] X.Q. Peng, H.F. Zhou, Y.Y. Lu, J.K. Chen, H.T. Wan, Y.Y. Zhang, Protective effects of Yinhuapinggan granule on mice with influenza viral pneumonia, Int. Immunopharm. 30 (2016) 85–93, https://doi.org/10.1016/j.intimp.2015.11.029.
[25] X.Q. Peng, H.F. Zhou, Y.Y. Zhang, J.H. Yang, H.T. Wan, Y. He, Antiviral effects of Yinhuapinggan granule against influenza virus infection in the ICR mice model, J. Nat. Med. 70 (1) (2016) 75–88, https://doi.org/10.1007/s11418-015-0939-z.
[26] L. Jin, Y.M. Zhang, J.H. Yang, H.F. Zhou, G.Z. Jia, Y. He, et al., Investigation of pharmacological mechanisms of yinhua pinggan granule on the treatment of pneumonia through network pharmacology and in vitro, BioMed Res. Int. 2022 (2022), 1602447, https://doi.org/10.1155/2022/1602447.
[27] S. Tansho-Nagakawa, Y. Sato, T. Ubagai, T. Kikuchi-Ueda, G.O. Kamoshida, S. Nishida, et al., Histopathological analysis of acinetobacter baumannii lung infection in a mouse model, Pol. J. Microbiol. 70 (4) (2021) 469–477, https://doi.org/10.33073/pjm-2021-044.
[28] E. Wahlström, A. Ollerstam, L. Sundius, H. Zhang, Use of lung weight as biomarker for assessment of lung toxicity in rat inhalation studies, Toxicol. Pathol. 41 (6) (2013) 902–912, https://doi.org/10.1177/0192623312470763.
[29] P. Aghasafari, U. George, R. Pidaparti, A review of inflammatory mechanism in airway diseases, Inflamm. Res. 68 (1) (2019) 59–74, https://doi.org/10.1007/s00011-018-1191-2.
[30] R. Karki, T.D. Kanneganti, The 'cytokine storm': molecular mechanisms and therapeutic prospects, Trends Immunol. 42 (8) (2021) 681–705, https://doi.org/10.1016/j.it.2021.06.001.
[31] S. Pires, D. Parker, Innate immune responses to acinetobacter baumannii in the airway, J. Interferon Cytokine Res. 39 (8) (2019) 441–449, https://doi.org/10.1089/jir.2019.0008.
[32] H. van Faassen, R. KuoLee, G. Harris, X. Zhao, J.W. Conlan, W. Chen, Neutrophils play an important role in host resistance to respiratory infection with Acinetobacter baumannii in mice, Infect. Immun. 75 (12) (2007) 5597–5608, https://doi.org/10.1128/IAI.00762-07.
[33] Q. Li, Y. Cui, B. Xu, Y. Wang, F. Lv, Z. Li, et al., Main active components of Jiawei Gegen Qinlian decoction protects against ulcerative colitis under different dietary environments in a gut microbiota-dependent manner, Pharmacol. Res. 170 (2021), 105694, https://doi.org/10.1016/j.phrs.2021.105694.
[34] N. Kelley, D. Jeltema, Y. Duan, Y. He, The NLRP3 inflammasome: an overview of mechanisms of activation and regulation, Int. J. Mol. Sci. 20 (13) (2019) 3328, https://doi.org/10.3390/ijms20133328.
[35] M.J. McVey, B.E. Steinberg, N.M. Goldenberg, Inflammasome activation in acute lung injury, Am. J. Physiol. Lung Cell Mol. Physiol. 320 (2) (2021) L165–L178, https://doi.org/10.1152/ajplung.00303.2020.
[36] Z. Zhong, A. Umemura, E. Sanchez-Lopez, S. Liang, S. Shalapour, J. Wong, et al., NF-κB restricts inflammasome activation via elimination of damaged mitochondria, Cell 164 (5) (2016) 896–910, https://doi.org/10.1016/j.cell.2015.12.057.
[37] H. Antushevich, Interplays between inflammasomes and viruses, bacteria (pathogenic and probiotic), yeasts and parasites, Immunol. Lett. 228 (2020) 1–14, https://doi.org/10.1016/j.imlet.2020.09.004.
[38] S. Christgen, T.D. Kanneganti, Inflammasomes and the fine line between defense and disease, Curr. Opin. Immunol. 62 (2020) 39–44, https://doi.org/10.1016/j.coi.2019.11.007.
[39] Y. Huang, W. Xu, R. Zhou, NLRP3 inflammasome activation and cell death, Cell. Mol. Immunol. 18 (9) (2021) 2114–2127, https://doi.org/10.1038/s41423-021-00740-6.